Computers, Materials & Continua CMC, vol.64, no.2, pp.1005-1023, 2020

New Three-Dimensional Assessment Model and Optimization of Acoustic Positioning System

Lin Zhao[1], Xiaobo Chen[1, 2, *], Jianhua Cheng[1], Lianhua Yu[3], Chengcai Lv[4] and Jiuru Wang[5]

Abstract: This paper addresses the problem of assessing and optimizing the acoustic positioning system for underwater target localization with range measurement. We present a new three-dimensional assessment model to evaluate the optimal geometric beacon formation whether meets user requirements. For mathematical tractability, it is assumed that the measurements of the range between the target and beacons are corrupted with white Gaussian noise with variance, which is distance-dependent. Then, the relationship between DOP parameters and positioning accuracy can be derived by adopting dilution of precision (DOP) parameters in the assessment model. In addition, the optimal geometric beacon formation yielding the best performance can be achieved via minimizing the values of geometric dilution of precision (GDOP) in the case where the target position is known and fixed. Next, in order to ensure that the estimated positioning accuracy on the region of interest satisfies the precision required by the user, geometric positioning accuracy (GPA), horizontal positioning accuracy (HPA) and vertical positioning accuracy (VPA) are utilized to assess the optimal geometric beacon formation. Simulation examples are designed to illustrate the exactness of the conclusion. Unlike other work that only uses GDOP to optimize the formation and cannot assess the performance of the specified size, this new three-dimensional assessment model can evaluate the optimal geometric beacon formation for each dimension of any point in three-dimensional space, which can provide guidance to optimize the performance of each specified dimension.

Keywords: Acoustic positioning system, three-dimensional assessment model, positioning accuracy, DOP, optimal configuration.

[1] College of Automation, Harbin Engineering University, Harbin, 150001, China.

[2] Department of Electrical and Electronic Engineering, The University of Melbourne, Victoria, 3010, Australia.

[3] College of Information and Communication, Harbin Engineering University, Harbin, 150001, China.

[4] Institute of Deep-Sea Science and Engineering, Chinese Academy of Sciences, Sanya, 572000, China.

[5] School of Information Science and Engineering, Linyi University, Linyi, 276005, China.

[*] Corresponding Author: Xiaobo Chen. Email: cxiaobo@hotmail.com.

Received: 24 February 2020; Accepted: 14 April 2020.

1 Introduction

The last decade has witnessed tremendous progress in the development of marine technology. In the execution of individual and military affairs, marine robotics, for example, autonomous underwater vehicle (AUV) and remote operated vehicle (ROV) are becoming ubiquitous. Reliable, accurate underwater positioning and navigation systems are quite important to the operation of AUV and ROV. Underwater positioning and navigation systems mainly include inertial navigation system [Xu, He, Qin et al. (2017); Chang, Li and Xue (2017)], geophysical navigation system [Rice, Kelmenson and Mendelsohn (2006); Teixeira (2013)], visual navigation system [Bonin-Font, Ortiz and Oliver (2008); Eustice, Pizarro and Singh (2008)], acoustic positioning system [Cheng, Shu and Liang (2008); Bayat, Crasta, Aguiar et al. (2016)] and integrated navigation system [Zhang, Chen and Li (2016); Shabani, Gholami and Davari (2014)]. To locate targets in a large range moving for a long time, the acoustic positioning system is always utilized. There are many researchers interested in solving the problem of how to place beacons in two or three dimensions. Zhang [Zhang (1995)] addressed the problem of determining the optimal two-dimensional spatial placement of multiple sensors participating in robot perception tasks. Levanon [Levanon (2000)] studied position determination in a two-dimensional scenario by achieving the lowest GDOP when range measured from beacons optimally located at the vertices of a regular n-sided polygon to the target. It can be noted that the definition of GDOP contains the fundamental relationship between measurement errors and computed position and time bias errors [Rob, Ronald, Christopher et al. (2006)]. In this paper, the definition of dilution of precision (DOP) is similar to that in Rob et al. [Rob, Ronald, Christopher et al. (2006)]. Moreno-Salinas et al. [Moreno-Salinas, Pascoal and Aranda (2013)] studied the multiple target localization with range measurements in unconstrained two-dimensional scenarios. Some other works also focused on three-dimensional scenarios. Sonia et al. [Sonia and Francesco (2006)] studied optimal sensor placement and motion coordination strategies for mobile sensor networks. They investigated the determinant of the fisher information matrix (FIM) in the two-dimensional and three-dimensional cases. In order to determine the sensor configuration that yields the most accurate positioning, the latter work was conducted to maximize FIM its determinant [Moreno-Salinas, Pascoal, Alcocer et al. (2010)]. Moreno-Salinas et al. [Moreno-Salinas, Pascoal and Aranda (2011, 2013, 2014, 2016)], Zhang et al. [Zhang, Chen and Li (2019)], Xue et al. [Xue, Xu, Yu et al. (2018)] and Su et al. [Su, Sheng and Xie (2019); Su, Sheng, Liu et al. (2019); Su, Sheng, Leung et al. (2019); Su, Sheng, Liu et al. (2020)] also had closely related work. More recently, Zou et al. [Zou, Wang, Zhu et al. (2016)] assumed that range measurements had different weights depending on their value and took uncertainty of initial node position into consideration for the calculation of the determinant of FIM. All the above researches focused on the optimal beacon configuration, and only few concentrated on the assessment models and rules of acoustic positioning system like assessment models and rules of global navigation satellite system (GNSS). For instance, in the work of Wang et al. [Wang, Lv and Li (2013)], the assessment models and rules of GNSS interoperability with range measurements were previously presented by the authors. Assessment parameters such as DOP, navigation satellite system precision and navigation satellite system integrity were introduced to assess the GNSS performance. Rajasekhar et al.

[Rajasekhar, Dutt and Rao (2016)] presented a study on GPS combined with Indian regional navigation satellite system (IRNSS) with DOP to measure the satellite-receiver geometry related to positioning accuracy. Also, Swaszek et al. [Swaszek, Hartnett and Seals (2017)] analyzed lower bounds DOP to allow users to assess how well their receivers are performing respecting the best possible performance, which should be useful for users to select satellites with multiple GNSS constellations.

Inspired by the previous works in the area, we offer the analytic assessment model of DOP parameters related to the position accuracy for the problem of evaluating acoustic positioning systems in this paper. Then, the geometric beacon placement is optimized based on target to beacons range measurements. Next, we require to focus on the values of GPA, HPA and VPA over the interesting region where the sampling points taking place of the target. The document is organized as follows. In Section 2, DOP parameters and positioning accuracy for the assessment model are derived, and the steps to assess the acoustic positioning system are listed as well. Section 3 contains the optimal beacon configurations for the case where the beacons can be placed freely in both two-dimensional scenario and three-dimensional scenario. The results of Section 3 are then examined in Section 4 for the particular scenario, and the steps to assess the acoustic positioning system in practice are shown. Finally, Section 5 includes conclusions and further research.

2 Assessment model: DOP parameters and position accuracy

The DOP parameters in Rob et al. [Rob, Ronald, Christopher et al. (2006)] are defined as geometry factors that relate the target position errors to the measurements of the ranges errors. Generally, the receiver and beacons clock both have bias errors from the system time and the bias errors are about a few microseconds, and the speed of sound in water is about 1500 m/s. Consequently, the measurements errors are insignificant compared to the accuracy of positioning and the DOP parameters in this paper do not consider the clock bias errors.

Next, the position of the *i*th beacon is (x_i, y_i, z_i) relative to the coordinate origin, and the actual position coordinates (x, y, z) of the target are considered unknown. In order to achieve the position of the target in three dimensions, ideal measurements of ranges are made with n (n>3) beacons from equations:

$$d_i = f(x,y,z) = \sqrt{(x_i - x)^2 + (y_i - y)^2 + (z_i - z)^2} \tag{1}$$

where d_i is the ideal measurement of range from the *i*th beacon to the target without noise interference, i ranges from 1 to n and references the beacons.

However, the measurements are always corrupted by noise. We assume that all noise sources are independent and have equal variance. Using this notation, the measurement model is given by:

$$D_i = \sqrt{(x_i - x)^2 + (y_i - y)^2 + (z_i - z)^2} + \omega_i \tag{2}$$

where *Di* is the actual measurement of range from the *i*th beacon to the target with noise interference, ω_i is the measurement error taken to be a zero mean Gaussian process

$N(0,\sigma^2)$ with covariance is σ^2.

Assuming that the position of the target is approximately estimated as (x_e, y_e, z_e) when the measurements are corrupted by noise. However, we still use Eq. (1) to estimate the position of the target, and so we can obtain the expression as follows:

$$D_i = f(x_e, y_e, z_e) = \sqrt{(x_i - x)^2 + (y_i - y)^2 + (z_i - z)^2} \tag{3}$$

We can denote the offset of the actual position (x, y, z) from the approximate position by a displacement $(\Delta x, \Delta y, \Delta z)$:

$$x = x_e + \Delta x, \quad y = y_e + \Delta y, \quad z = z_e + \Delta z \tag{4}$$

Substituting Eq. (4) into Eq. (1), we can attain the expression:

$$f(x, y, z) = f(x_e + \Delta x, y_e + \Delta y, z_e + \Delta z) \tag{5}$$

The function in the right of Eq. (5) can be expanded about the approximate target's position using a Taylor series:

$$\begin{aligned} &f(x_e + \Delta x, y_e + \Delta y, z_e + \Delta z) = f(x_e, y_e, z_e) + \\ &\frac{\partial f(x_e, y_e, z_e)}{\partial x_e}\Delta x + \frac{f(x_e, y_e, z_e)}{\partial y_e}\Delta y + \frac{\partial f(x_e, y_e, z_e)}{\partial z_e}\Delta z \end{aligned} \tag{6}$$

The expansion has been truncated after the first-order partial derivatives and the partial derivatives evaluate as follows:

$$\begin{aligned} &\frac{\partial f(x_e, y_e, z_e)}{\partial x_e} = -\frac{(x_i - x_e)}{D_i} \\ &\frac{f(x_e, y_e, z_e)}{\partial y_e} = -\frac{(y_i - y_e)}{D_i} \\ &\frac{\partial f(x_e, y_e, z_e)}{\partial z_e} = -\frac{(z_i - z_e)}{D_i} \end{aligned} \tag{7}$$

Substituting Eq. (7) into Eq. (6) yields:

$$d_i = D_i - \frac{(x_i - x_e)}{D_i}\Delta x - \frac{(y_i - y_e)}{D_i}\Delta y - \frac{(z_i - z_e)}{D_i}\Delta z \tag{8}$$

For convenience, we will simplify Eq. (8) by introducing new variables, where:

$$a_{xi} = \frac{(x_i - x_e)}{D_i}, \quad a_{yi} = \frac{(y_i - y_e)}{D_i}, \quad a_{zi} = \frac{(z_i - z_e)}{D_i} \tag{9}$$

By substituting Eq. (9) into Eq. (8), it gives:

$$\omega_i = D_i - d_i = a_{xi}\Delta x + a_{yi}\Delta y + a_{zi}\Delta z \tag{10}$$

Now, the three unknowns composing the vector $\Delta\mathbf{u} = (\Delta x, \Delta y, \Delta z)^{\mathrm{T}}$ and the unknown quantities can be determined by solving the matrix, which can be shown as:

$$\Delta\mathbf{d} = \mathbf{H}\Delta\mathbf{u} \tag{11}$$

where T donates the transpose of matrix; the matrix $\Delta\mathbf{d}$ and observation matrix $\mathbf{H}$ are described by making the definitions:

$$\Delta\mathbf{d} = \begin{bmatrix} \omega_1 \\ \omega_2 \\ \vdots \\ \omega_n \end{bmatrix} \tag{12}$$

$$\mathbf{H} = \begin{bmatrix} a_{x1} & a_{y1} & a_{z1} \\ a_{x2} & a_{y2} & a_{z2} \\ \vdots & \vdots & \vdots \\ a_{xn} & a_{yn} & a_{zn} \end{bmatrix} \tag{13}$$

If vectors (a_{xi}, a_{yi}, a_{zi}) do not all lie in a plane, the weighting matrix $(\mathbf{H}^{\mathrm{T}}\mathbf{H})$ will be invertible. Thus, the method of least squares can be used to solve Eq. (11) for $\Delta\mathbf{u}$:

$$\Delta\mathbf{u} = (\mathbf{H}^{\mathrm{T}}\mathbf{H})^{-1}\mathbf{H}^{\mathrm{T}}\Delta\mathbf{d} \tag{14}$$

In fact, the ideal positioning accuracy is decided by $\Delta\mathbf{u}$, and then the covariance of $\Delta\mathbf{u}$ is obtained by forming the product and computing an expected value $\Delta\mathbf{u}\Delta\mathbf{u}^{\mathrm{T}}$:

$$\begin{aligned} \operatorname{cov}\Delta\mathbf{u} &= \mathrm{E}[\Delta\mathbf{u}\Delta\mathbf{u}^{\mathrm{T}}] = \left[(\mathbf{H}^{\mathrm{T}}\mathbf{H})^{-1}\mathbf{H}^{\mathrm{T}}\Delta\mathbf{d}\left((\mathbf{H}^{\mathrm{T}}\mathbf{H})^{-1}\mathbf{H}^{\mathrm{T}}\Delta\mathbf{d}\right)^{\mathrm{T}} \right] \\ &= \left[(\mathbf{H}^{\mathrm{T}}\mathbf{H})^{-1}\mathbf{H}^{\mathrm{T}}\Delta\mathbf{d}\Delta\mathbf{d}^{\mathrm{T}}\mathbf{H}(\mathbf{H}^{\mathrm{T}}\mathbf{H})^{-1} \right] = (\mathbf{H}^{\mathrm{T}}\mathbf{H})^{-1}\mathbf{H}^{\mathrm{T}}\operatorname{cov}(\Delta\mathbf{d})\mathbf{H}(\mathbf{H}^{\mathrm{T}}\mathbf{H})^{-1} \end{aligned} \tag{15}$$

The usual assumption is that ω_{i} is distributed and independent, with zero mean Gaussian process whose variance is σ^2. The covariance of $\Delta\mathbf{d}$ is a scalar multiple of the identity: $\sigma^2\mathbf{I}_{n\times n}$, where $\mathbf{I}_{n\times n}$ is the $n\times n$ identity matrix. Thus, the result of Eq. (15) can be derived as:

$$\operatorname{cov}\Delta\mathbf{u} = \sigma^2(\mathbf{H}^{\mathrm{T}}\mathbf{H})^{-1}\mathbf{H}^{\mathrm{T}}\mathbf{H}(\mathbf{H}^{\mathrm{T}}\mathbf{H})^{-1} = \sigma^2(\mathbf{H}^{\mathrm{T}}\mathbf{H})^{-1} \tag{16}$$

Under the stated assumptions, the covariance of the errors of the position is just a scalar multiple of the weighting matrix $(\mathbf{H}^{\mathrm{T}}\mathbf{H})^{-1}$. The covariance of $\Delta\mathbf{u}$ is a 3×3 matrix and has an expanded representation:

$$\operatorname{cov}\Delta\mathbf{u} = \begin{bmatrix} \sigma_x^2 & \sigma_x\sigma_y & \sigma_x\sigma_z \\ \sigma_x\sigma_y & \sigma_y^2 & \sigma_y\sigma_z \\ \sigma_x\sigma_z & \sigma_y\sigma_z & \sigma_z^2 \end{bmatrix} \tag{17}$$

The components of the weighting matrix $(\mathbf{H}^{\mathrm{T}}\mathbf{H})^{-1}$ quantify how measurement errors translate into components of the covariance of $\Delta\mathbf{u}$. The weighting matrix $(\mathbf{H}^{\mathrm{T}}\mathbf{H})^{-1}$ can be expressed in a component form:

$$(\mathbf{H}^T\mathbf{H})^{-1} = \mathbf{D} = \begin{bmatrix} D_{11} & D_{12} & D_{13} \\ D_{21} & D_{22} & D_{23} \\ D_{31} & D_{32} & D_{33} \end{bmatrix} \tag{18}$$

Unlike other work that only uses GDOP to optimize the formation, which cannot assess the performance of any specified dimensions, more DOP parameters are presented in this paper, and GDOP, HDOP and VDOP are utilized to assess the optimal geometric beacon formation in each dimension for any point in three-dimensional space:

$$\begin{aligned} \text{GDOP} &= \sqrt{D_{11} + D_{22} + D_{33}} = \frac{\sqrt{\sigma_x^2 + \sigma_y^2 + \sigma_z^2}}{\sigma} \\ \text{HDOP} &= \sqrt{D_{11} + D_{22}} = \frac{\sqrt{\sigma_x^2 + \sigma_y^2}}{\sigma} \\ \text{VDOP} &= \sqrt{D_{33}} = \frac{\sqrt{\sigma_z^2}}{\sigma} \end{aligned} \tag{19}$$

To assess the acoustic positioning system, the sampling points over interesting region are adopted to take place of the approximate position of the target. Next, the observation matrix **H** is achieved by Eq. (20):

$$\mathbf{H} = \begin{bmatrix} \frac{x_1 - x_s}{r_1} & \frac{y_1 - y_s}{r_1} & \frac{z_1 - z_s}{r_1} \\ \frac{x_2 - x_s}{r_2} & \frac{y_2 - y_s}{r_2} & \frac{z_2 - x_s}{r_2} \\ \vdots & \vdots & \vdots \\ \frac{x_n - x_s}{r_n} & \frac{y_n - y_s}{r_n} & \frac{z_n - z_s}{r_n} \end{bmatrix} \tag{20}$$

where (x_i, y_i, z_i), i=1$\cdots n$ denotes the position of the ith beacon in three dimensions, (x_s, y_s, z_s) denotes the sampling point position over interesting region in three dimensions, ri is the range between the ith beacon and the sampling point.

Eq. (20) is valid and provides that the range measurement errors are sufficiently small, so that the error between the actual position of the sample point and approximately estimated position can be ignored. The minimum of σ is $c/2f$ in theory, where c is the speed of propagation of sound in the water, f is the frequency of sound in the water. However, σ in practice is always far larger than $c/2f$. Multiply σ by GDOP, HDOP and VDOP, respectively, so GPA, HPA and VPA will be obtained, correspondingly.

$$\begin{aligned} \text{GPA} &= \sqrt{\sigma_x^2 + \sigma_y^2 + \sigma_z^2} = \text{GDOP} \times \sigma \\ \text{HPA} &= \sqrt{\sigma_x^2 + \sigma_y^2} = \text{HDOP} \times \sigma \\ \text{VPA} &= \sigma_z = \text{VDOP} \times \sigma \end{aligned} \tag{21}$$

Compare GPA, HPA and VPA with the user requirements and decide whether the

positioning accuracy meets the user requirements. If they cannot satisfy the needs, it means more beacons are required, e.g., add the beacons in the horizontal plane of HPA, add the beacons in the vertical plane for VPA, and add the beacons in main horizontal plane fir GPA.

According to the above analysis, the steps to assessment acoustic positioning system can be summarized as follows:

1. Determine the optimal beacons configurations with *n* beacons: the beacons should be distributed at the vertices of a regular *n*-sided polygon on the same plane. This conclusion can be brought in Section 3.
2. According to the spatial resolution needed by users, the sampling points should be ensured in space, then compute the ranges from beacons to all sampling points in space by Eq. (1).
3. Define the variance of range measurements errors σ, obtain the DOP parameters, GDOP, HDOP and VDOP by Eq. (19), and compute the GPA, HPA and VPA by Eq. (21).
4. Determine whether increase the number of beacons into the acoustic positioning system according to the comparison between the ideal positioning accuracy and the requirements of users.

3 The optimal beacons configurations with DOP parameters

3.1 Two-dimensional scenarios

This section addresses the problem of estimating beacon placement for underwater target positioning in two-dimensional space under the condition that the beacons and the sampling point are on the horizontal plane. In this situation, **H** is singular, so the matrix **D** does not exist. To simplify without loss of generality, the sampling point is regarded as the origin in the inertial coordinate frame hereinafter. It is assumed that the position of the *i*th beacon is located on the point whose radius is r_i and the polar angle is α_i, so the polar coordinate of the *i*th beacon is ($r_i \cos\alpha_i$, $r_i \sin\alpha_i$), while the matrix **H** can be simplified as $\mathbf{H}_1$:

$$\mathbf{H}_1 = \begin{bmatrix} \dfrac{r_1\cos\alpha_1}{r_1} & \dfrac{r_1\sin\alpha_1}{r_1} \\ \dfrac{r_2\cos\alpha_2}{r_2} & \dfrac{r_2\sin\alpha_2}{r_2} \\ \vdots & \vdots \\ \dfrac{r_n\cos\alpha_n}{r_n} & \dfrac{r_n\sin\alpha_n}{r_n} \end{bmatrix} = \begin{bmatrix} \cos\alpha_1 & \sin\alpha_1 \\ \cos\alpha_2 & \sin\alpha_2 \\ \vdots & \vdots \\ \cos\alpha_2 & \sin\alpha_n \end{bmatrix} \tag{22}$$

At this point, the vectors of **X** and **Y** can be defined as:

$$\begin{aligned} \mathbf{X} &= \begin{bmatrix} \cos\alpha_1 & \cos\alpha_2 & \cdots & \cos\alpha_n \end{bmatrix} \\ \mathbf{Y} &= \begin{bmatrix} \sin\alpha_1 & \sin\alpha_2 & \cdots & \sin\alpha_n \end{bmatrix} \end{aligned} \tag{23}$$

It can be obviously seen that the analytical relationship of the determinant of **X** and **Y** is as follows:

$$|\mathbf{X}|^2 + |\mathbf{Y}|^2 = n \tag{24}$$

As a consequence, f can be defined as the angle formed by vectors **X** and **Y**, and the weighting matrix $\mathbf{D}_1 = (\mathbf{H}_1{}^{\mathrm{T}}\mathbf{H}_1)^{-1}$ is parameterized by two vectors **X** and **Y**:

$$\mathbf{D}_1 = \begin{bmatrix} \sum_{i=1}^{n}\cos^2\alpha_i & \sum_{i=1}^{n}\cos\alpha_i\sin\alpha_i \\ \sum_{i=1}^{n}\cos\alpha_i\sin\alpha_i & \sum_{i=1}^{n}\sin^2\alpha_i \end{bmatrix}^{-1} = \frac{\begin{bmatrix} \mathbf{Y}^2 & -|\mathbf{Y}||\mathbf{X}|\cos\phi \\ -|\mathbf{Y}||\mathbf{X}|\cos\phi & \mathbf{X}^2 \end{bmatrix}}{\det(\mathbf{H}_1{}^{\mathrm{T}}\mathbf{H}_1)} \tag{25}$$

The determinant of $\mathbf{H}_1{}^{\mathrm{T}}\mathbf{H}_1$ yields:

$$\det(\mathbf{H}_1{}^{\mathrm{T}}\mathbf{H}_1) = |\mathbf{Y}||\mathbf{X}|(1-\cos^2\phi) \tag{26}$$

Correspondingly, $\cos^2\phi = 0$ is the only feasible solution to make the $\det(\mathbf{H}_1{}^{\mathrm{T}}\mathbf{H}_1)$ largest that implies that vectors **X** and **Y** are orthogonal. This condition makes $\mathbf{H}_1{}^{\mathrm{T}}\mathbf{H}_1$ be a diagonal matrix and $\det(\mathbf{H}_1{}^{\mathrm{T}}\mathbf{H}_1)$, which can be written as:

$$\det(\mathbf{H}_1{}^{\mathrm{T}}\mathbf{H}_1) = |\mathbf{Y}|^2|\mathbf{X}|^2 = |\mathbf{X}|^2(n-|\mathbf{X}|^2) \le -(|\mathbf{X}|^2 - n/2)^2 + n^2/4 \tag{27}$$

Finally, we can get Eq. (28):

$$\mathrm{HDOP} \ge \sqrt{\frac{n}{n^2/4}} = \sqrt{\frac{4}{n}} \tag{28}$$

We now need to ensure the beacon configurations. The sampling point needs to be defined at the center of an *n*-sided regular polygon ($n \ge 2$), and the n beacons are placed at the vertices of a regular *n*-sided polygon. Next, the coordinate of the *i*th beacon is described as:

$$\left(r_i\cos\frac{2\pi(i-1)}{n}, r_i\sin\frac{2\pi(i-1)}{n}\right) i = 1,2,\cdots,n \tag{29}$$

Then, the matrix $\mathbf{H}_1$ can be described as:

$$\mathbf{H}_1 = \begin{bmatrix} \cos 0 & \sin 0 \\ \cos\frac{2\pi}{n} & \sin\frac{2\pi}{n} \\ \vdots & \vdots \\ \cos\frac{2\pi(i-1)}{n} & \sin\frac{2\pi(i-1)}{n} \end{bmatrix} \tag{30}$$

With the Fourier summation formulas:

$$\sum_{i=1}^{n}\cos^2\frac{2\pi(i-1)}{n}=\sum_{i=1}^{n}\sin^2\frac{2\pi(i-1)}{n}=\frac{n}{2}$$
$$\sum_{i=1}^{n}\cos\frac{2\pi(i-1)}{n}\sin\frac{2\pi(i-1)}{n}=0 \tag{31}$$
$$\sum_{i=1}^{n}\cos\frac{2\pi(i-1)}{n}=\sum_{i=1}^{n}\sin\frac{2\pi(i-1)}{n}=0$$

Substituting Eq. (31) into Eq. (25) yields:

$$\mathbf{D}_1=\begin{bmatrix}\frac{n}{2} & 0\\ 0 & \frac{n}{2}\end{bmatrix}^{-1}=\begin{bmatrix}\frac{2}{n} & 0\\ 0 & \frac{2}{n}\end{bmatrix} \tag{32}$$

It can be concluded that in two-dimensional scenarios, it is clear that the beacon configurations have no explicit dependence on the ranges, only related to the angles that the range vectors form with the unit axes of the frame. Moreover, for position determination, based on n range measurements (n>2), the lowest possible HDOP is $2/\sqrt{n}$. This value will occur when the sampling point is on the initial point, and the n beacons are located at the vertices of regular n-sided polygon. Besides, more optimal beacon configurations can be generated by two methods: 1) multiplying the range of each beacon to the sampling point by an arbitrary positive number as long as the sampling point could receive the signals from all beacons. 2) rotating the beacon formation rigidly in terms of an arbitrary axis. However, these two approaches can only achieve the lowest possible HDOP constant when the sampling point is on the initial point, and the n beacons are located at the vertices of regular n-sided polygon.

3.2 Three-dimensional scenarios

Similar to the two-dimensional scenarios, the sampling point is considered to be located at the origin of the inertial coordinate frame hereinafter. Assume that the position of the ith beacon is located on the point (x_i, y_i, z_i), and the range between the sampling point and the beacon is $r_i=\sqrt{x_i^2+y_i^2+z_i^2}$. The angles $(\alpha_i,\beta_i,\gamma_i)$ can be defined as Eq. (33):

$$\begin{aligned}\cos\alpha_i &= x_i/r_i\\ \cos\beta_i &= y_i/r_i\\ \cos\gamma_i &= z_i/r_i\end{aligned} \tag{33}$$

The coordinate of the ith beacon can be defined as $(r_i\cos\alpha_i, r_i\cos\beta_i, r_i\cos\gamma_i)$, and the matrix of **H** becomes:

$$\mathbf{H}_1 = \begin{bmatrix} \cos\alpha_1 & \cos\beta_1 & \cos\gamma_1 \\ \cos\alpha_2 & \cos\beta_2 & \cos\gamma_2 \\ \vdots & \vdots & \vdots \\ \cos\alpha_n & \cos\beta_n & \cos\gamma_n \end{bmatrix} \tag{34}$$

It is convenient to introduce the vectors **X**, **Y** and **Z** as:

$$\begin{aligned} \mathbf{X} &= \begin{bmatrix} \cos\alpha_1 & \cos\alpha_2 & \cdots & \cos\alpha_n \end{bmatrix} \\ \mathbf{Y} &= \begin{bmatrix} \cos\beta_1 & \cos\beta_2 & \cdots & \cos\beta_n \end{bmatrix} \\ \mathbf{Z} &= \begin{bmatrix} \cos\gamma_1 & \cos\gamma_2 & \cdots & \cos\gamma_n \end{bmatrix} \end{aligned} \tag{35}$$

The relationship of the determinant of **X**, **Y** and **Z** is shown as follows:

$$|\mathbf{X}|^2 + |\mathbf{Y}|^2 + |\mathbf{Z}|^2 = n \tag{36}$$

Thus, Eq. (18) can be rewritten as:

$$\mathbf{D} = (\mathbf{H}^T\mathbf{H})^{-1} = \begin{bmatrix} |\mathbf{X}|^2 & |\mathbf{X}||\mathbf{Y}|\cos\varphi & |\mathbf{X}||\mathbf{Z}|\cos\theta \\ |\mathbf{X}||\mathbf{Y}|\cos\varphi & |\mathbf{Y}|^2 & |\mathbf{Y}||\mathbf{Z}|\cos\omega \\ |\mathbf{X}||\mathbf{Z}|\cos\theta & |\mathbf{Y}||\mathbf{Z}|\cos\omega & |\mathbf{Z}|^2 \end{bmatrix}^{-1} \tag{37}$$

where φ, θ and ω are the angles formed by vectors **X**, **Y** and **Z**, respectively. From Eq. (37), it follows that:

$$\mathrm{GDOP} = \sqrt{\frac{|\mathbf{Y}|^2|\mathbf{Z}|^2(1-\cos^2\omega) + |\mathbf{X}|^2|\mathbf{Z}|^2(1-\cos^2\theta) + |\mathbf{X}|^2|\mathbf{Y}|^2(1-\cos^2\varphi)}{\det(\mathbf{H}^{\mathrm{T}}\mathbf{H})}} \tag{38}$$

The determinant of $\mathbf{H}^{\mathrm{T}}\mathbf{H}$ yields:

$$\det(\mathbf{H}^{\mathrm{T}}\mathbf{H}) = |\mathbf{X}|^2|\mathbf{Y}|^2|\mathbf{Z}|^2(1 + 2\cos\omega\cos\theta\cos\varphi - \cos^2\theta - \cos^2\omega - \cos^2\varphi) \tag{39}$$

We suppose a procedure inspired in the two-dimensional problem; the optimal solution is:

$$\cos\omega = \cos\theta = \cos\varphi = 0 \tag{40}$$

In this situation, it follows that:

$$\begin{aligned} \frac{1-\cos^2\omega}{1 + 2\cos\omega\cos\theta\cos\varphi - \cos^2\theta - \cos^2\omega - \cos^2\varphi} &= 1 \\ \frac{1-\cos^2\theta}{1 + 2\cos\omega\cos\theta\cos\varphi - \cos^2\theta - \cos^2\omega - \cos^2\varphi} &= 1 \\ \frac{1-\cos^2\varphi}{1 + 2\cos\omega\cos\theta\cos\varphi - \cos^2\theta - \cos^2\omega - \cos^2\varphi} &= 1 \end{aligned} \tag{41}$$

It can be demonstrated that 1 is the minimum possible value. Without loss of generality, a smaller value can be supposed to satisfy:

$$\frac{1-\cos^2\omega}{1+2\cos\omega\cos\theta\cos\varphi-\cos^2\theta-\cos^2\omega-\cos^2\varphi}<1 \tag{42}$$

Generally, the determinant of symmetrical matrix $\mathbf{H}^{\mathrm{T}}\mathbf{H}$ is not less than 0. Moreover, GDOP is inexistence when the determinant of $\mathbf{H}^{\mathrm{T}}\mathbf{H}=0$. Therefore, the determinant of $\mathbf{H}^{\mathrm{T}}\mathbf{H}>0$ is in consideration. In this situation, the above inequality is equivalent to:

$$2\cos\omega\cos\theta\cos\varphi-\cos^2\theta-\cos^2\varphi \tag{43}$$

Because $\left|\cos\omega\right|<1$, it follows that:

$$2\cos\omega\cos\theta\cos\varphi\le\cos^2\theta+\cos^2\varphi \tag{44}$$

This conclusion contradicts Eq. (43). Therefore:

$$\frac{1-\cos^2\omega}{1+2\cos\omega\cos\theta\cos\varphi-\cos^2\theta-\cos^2\omega-\cos^2\varphi}\ge1 \tag{45}$$

Similarly, we can prove that:

$$\begin{aligned}&\frac{1-\cos^2\theta}{1+2\cos\omega\cos\theta\cos\varphi-\cos^2\theta-\cos^2\omega-\cos^2\varphi}\ge1\\&\frac{1-\cos^2\varphi}{1+2\cos\omega\cos\theta\cos\varphi-\cos^2\theta-\cos^2\omega-\cos^2\varphi}\ge1\end{aligned} \tag{46}$$

In such circumstances, GDOP is computed as:

$$\mathrm{GDOP}=\sqrt{\frac{1}{\left|\mathbf{X}\right|^2}+\frac{1}{\left|\mathbf{Y}\right|^2}+\frac{1}{\left|\mathbf{Z}\right|^2}}=\sqrt{\frac{1}{\left|\mathbf{X}\right|^2}+\frac{1}{\left|\mathbf{Y}\right|^2}+\frac{1}{n-\left|\mathbf{X}\right|^2-\left|\mathbf{Y}\right|^2}} \tag{47}$$

The binary function $f(a,b)$ can be constructed as follows:

$$f(a,b)=\frac{1}{a}+\frac{1}{b}+\frac{1}{n-a-b} \tag{48}$$

The Hessian matrix of Eq. (48) is:

$$\mathrm{Hessian}=\begin{bmatrix}\dfrac{\partial^2 f(a,b)}{\partial a^2} & \dfrac{\partial f(a,b)}{\partial ab}\\ \dfrac{\partial f(a,b)}{\partial ab} & \dfrac{\partial^2 f(a,b)}{\partial b^2}\end{bmatrix}=\begin{bmatrix}\dfrac{2}{a^3}+\dfrac{2}{(n-a-b)^3} & \dfrac{2}{(n-a-b)^3}\\ \dfrac{2}{(n-a-b)^3} & \dfrac{2}{a^3}+\dfrac{2}{(n-a-b)^3}\end{bmatrix} \tag{49}$$

where it is easy to proof that the Hessian matrix of Eq. (48) is positive definite, the minimum value of $f(a,b)$ is obtained provided that the first derivatives equal to 0:

$$\begin{aligned}&\frac{\partial f(a,b)}{\partial a}=\frac{1}{(n-a-b)^2}-\frac{1}{a^2}=0\\&\frac{\partial f(a,b)}{\partial b}=\frac{1}{(n-a-b)^2}-\frac{1}{b^2}=0\end{aligned} \tag{50}$$

Having that:

$$a = b = \frac{n}{3} \tag{51}$$

Substituting this result in Eq. (36), we obtain:

$$|\mathbf{X}|^2 = |\mathbf{Y}|^2 = |\mathbf{Z}|^2 = \frac{n}{3} \tag{52}$$

Next, the geometric configuration can be established in three-dimensional scenarios. To simplify the computation, we assume that the optimal beacon formations are placed on a unit sphere centered at the sampling point. Inspired by the work in two-dimensional scenarios, we address the problem of optimal beacon placement subject to the condition that the beacons are on the same plane. Then, the beacons may be distributed at the vertices of a regular n-sided polygon, which belongs to the circumference of the plane $z = 1/\sqrt{3}$ or on the circumference of the plane $z = -1/\sqrt{3}$. In addition, the optimal radius. Next, a simple proof of this geometric configuration can be presented. Firstly, the positions of the beacons in polar coordinates can be rewritten as:

$$\begin{aligned} \cos\alpha_i &= x_i / r_i = x_i \\ \cos\beta_i &= y_i / r_i = y_i \\ \cos\gamma_i &= z_i / r_i = z_i \end{aligned} \tag{53}$$

Because all beacons are distributed on the circumference of the plane $z = 1/\sqrt{3}$ or on the circumference of the plane $z = -1/\sqrt{3}$, so it follows that:

$$\begin{aligned} &\cos^2\gamma_i = 1/3 \\ &|\mathbf{Z}|^2 = \sum_{i=1}^{n} \cos^2\gamma_i = n/3 \end{aligned} \tag{54}$$

With the conclusion in Eq. (31), we can get:

$$\begin{aligned} &\sum_{i=1}^{n} (x_i / R)^2 = \sum_{i=1}^{n} \cos^2 \frac{2\pi(i-1)}{n} = \frac{n}{2} \\ &\sum_{i=1}^{n} (y_i / R)^2 = \sum_{i=1}^{n} \sin^2 \frac{2\pi(i-1)}{n} = \frac{n}{2} \\ &\sum_{i=1}^{n} \left(\frac{x_i}{R}\right)\left(\frac{y_i}{R}\right) = \sum_{i=1}^{n} \cos\frac{2\pi(i-1)}{n} \sin\frac{2\pi(i-1)}{n} = 0 \\ &\sum_{i=1}^{n} \left(\frac{x_i}{R}\right) = \sum_{i=1}^{n} \cos\frac{2\pi(i-1)}{n} = 0 \\ &\sum_{i=1}^{n} \left(\frac{y_i}{R}\right) = \sum_{i=1}^{n} \sin\frac{2\pi(i-1)}{n} = 0 \end{aligned} \tag{55}$$

Therefore, we can obtain the formulas as follows:

$$
\begin{aligned}
|\mathbf{X}|^2 &= \sum_{i=1}^{n}(x_i)^2 = \frac{n}{2}\times R^2 = \frac{n}{3} \\
|\mathbf{Y}|^2 &= \sum_{i=1}^{n}(y_i)^2 = \frac{n}{2}\times R^2 = \frac{n}{3} \\
|\mathbf{X}||\mathbf{Y}| &= \sum_{i=1}^{n}(x_i y_i) = 0 \\
|\mathbf{X}||\mathbf{Z}| &= \sqrt{1/3}\sum_{i=1}^{n} x_i = 0 \\
|\mathbf{Y}||\mathbf{Z}| &= \sqrt{1/3}\sum_{i=1}^{n} y_i = 0
\end{aligned} \tag{56}
$$

Besides, Eq. (37) yields:

$$
\mathbf{D} = (\mathbf{H}^{\mathrm{T}}\mathbf{H})^{-1} = \begin{bmatrix} n/3 & 0 & 0 \\ 0 & n/3 & 0 \\ 0 & 0 & n/3 \end{bmatrix}^{-1} = \begin{bmatrix} 3/n & 0 & 0 \\ 0 & 3/n & 0 \\ 0 & 0 & 3/n \end{bmatrix} \tag{57}
$$

Once the optimal beacon placement on a unit sphere in three-dimensional scenarios is found in terms of the direction cosines achieved above, more infinite optimal beacon placements can be generated by multiplying the range of each beacon to the sampling point by an arbitrary positive number, as long as the sampling point can receive the signal from the beacons. The lowest possible GDOP is $3/\sqrt{n}$ based on the n range measurements (n>3).

An interesting problem arises: whether HDOP and VDOP can attain the lowest value when the optimal beacons configurations cause GDOP lowest. The answer is no. Assume that the coordinate of the ith beacon is (x_i, y_i, z_i), without loss of generality, if the beacons are located on a circle centered at the sampling point, which can be described as:

$$
x_i^2 + y_i^2 = \hat{r}^2 \tag{58}
$$

With the condition shown in Eqs. (36) and (40), HDOP and VDOP can be described as:

$$
\begin{aligned}
\mathrm{HDOP} &= \sqrt{\frac{1}{|\mathbf{X}|^2} + \frac{1}{|\mathbf{Y}|^2}} = \sqrt{\frac{n - n\dfrac{z^2}{\hat{r}^2 + z^2}}{\sum_{i=1}^{n}\dfrac{x_i^2}{\hat{r}^2 + z^2}\sum_{i=1}^{n}\dfrac{y_i^2}{\hat{r}^2 + z^2}}} \\
&= \sqrt{\frac{n(\hat{r}^2 + z^2)^2 - nz^2(\hat{r}^2 + z^2)}{\sum_{i=1}^{n} x_i^2 \sum_{i=1}^{n} y_i^2}} = \sqrt{\frac{n(\hat{r}^2 + z^2)^2 \hat{r}^2}{\sum_{i=1}^{n} x_i^2 \sum_{i=1}^{n} y_i^2}}
\end{aligned} \tag{59}
$$

$$
\mathrm{VDOP} = \sqrt{\frac{1}{|\mathbf{Z}|^2}} = \sqrt{\frac{1}{n\dfrac{z^2}{\hat{r}^2 + z^2}}} = \sqrt{\frac{1}{n}\left(1 + \frac{\hat{r}^2}{z^2}\right)} \tag{60}
$$

It can be demonstrated that the vertical distance z between beacons and sampling point becomes larger, HDOP will be larger, and VDOP will be smaller. In many practical applications of interest, however, the sampling point depth can be measured directly with

a small error. Thus, there is no need to estimate it with acoustic range measurements. Therefore, based on the GDOP or HDOP, we can decide whether the beacons configurations meet user needs.

4 Simulation examples

4.1 Optimal beacon placement in two-dimensional scenarios

If there is only one sampling point in the acoustic positioning system and is known to users, Section 3.1 clearly shows that the optimal beacons are placed at the vertices of regular n-sided polygon. Under the experimental conditions, it is necessary to estimate the positioning accuracy in term of the beacon formation for anywhere in the acoustic positioning system. To achieve this goal, HPA with hypothetical sampling point on a grid in a finite spatial region A is computed. In this paper, the region A will always be a rectangle. The formation is one in which four beacons are placed at p_1=[2000, 2000] m, p_2=[-2000, 2000] m, p_3=[-2000, -2000] m, p_4=[2000, -2000] m. It can be assumed that all range measurements are corrupted by additive zero mean Gaussian noise with variance σ=1 so that the values of HPA are equal to that of HDOP. The spatial resolution chosen is 2 m×2 m.

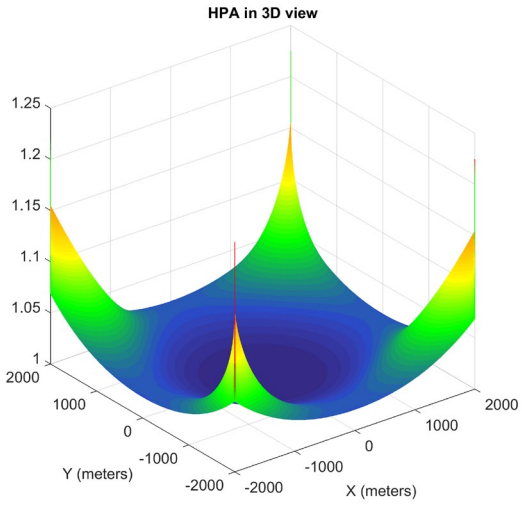

Figure 1: HPA in the 3D view in two-dimensional scenarios

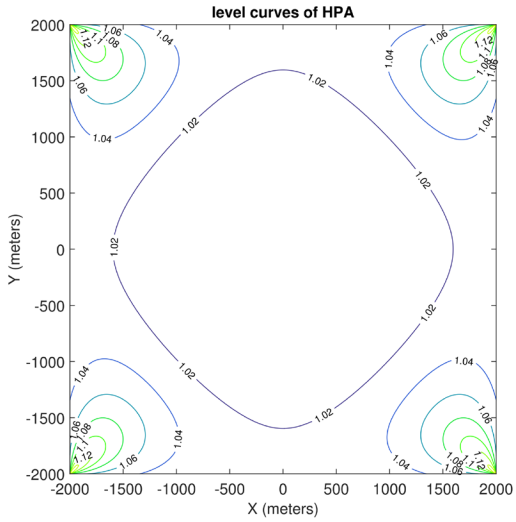

Figure 2: Level curves of HPA in two-dimensional scenarios

The simulation results of HPA are presented in Figs. 1 and 2. In Fig. 1, the values of HPA in 3D view for region A are shown. It is important to note that the HPA obtained at the point of beacon is computed with three other beacons, without the beacon location itself, so as to avoid $\det(\mathbf{H}^{\mathrm{T}}\mathbf{H})=0$. Thus, the values of HPA at these points are extra-large. In Fig. 2, the level curves of HPA in region A are indicated. We can draw the conclusion that the better performance obtained in two-dimensional scenarios is within the circle of 1.02, meaning that around the center of the beacon is more accurate than that nearby the beacon. Furthermore, the better positioning region in two-dimensional scenarios is like a square, but rotated 90 degrees to the beacon formation.

4.2 Optimal beacon placement in the three-dimensional scenario

For the three-dimensional scenario, the beacons are supposed to be placed on the surface of the sea, and the coordinates are p_1=[2000, 2000, 0] m, p_2=[-2000, 2000, 0] m, p_3=[-2000, -2000, 0] m, p_4=[2000, -2000, 0] m. Similar to the two-dimensional scenario, all range measurements are assumed to be corrupted by additive zero mean Gaussian noise with variance σ=1. The height of the sampling point at three different levels is taken into account in the computation of the GPA involved in the optimization figuration. The depths of the sampling points are assumed to be -1000 m, -2000 m and -3000 m, respectively. The spatial resolution chosen is 2 m×2 m. In Figs. 3 and 4, GPA values of the -2000 m sampling points are supplied. The other GPA values of the -1000 m and -3000 m sampling points are similar to those of -2000 m. They are not addressed in this paper due to space limitations. The comparisons of GPA, HPA and VPA between different heights of sampling points are provided in Tab. 1.

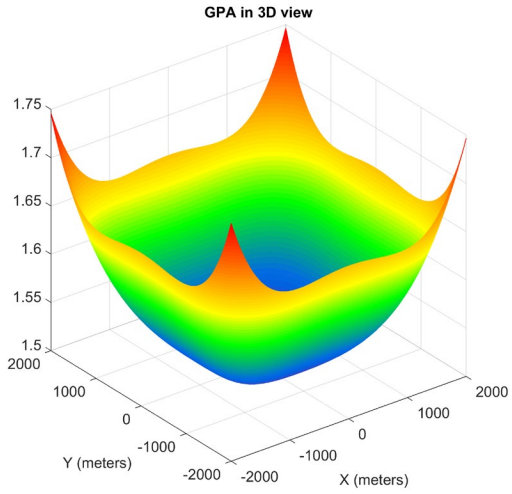

Figure 3: Level curves of HPA in three-dimensional scenarios

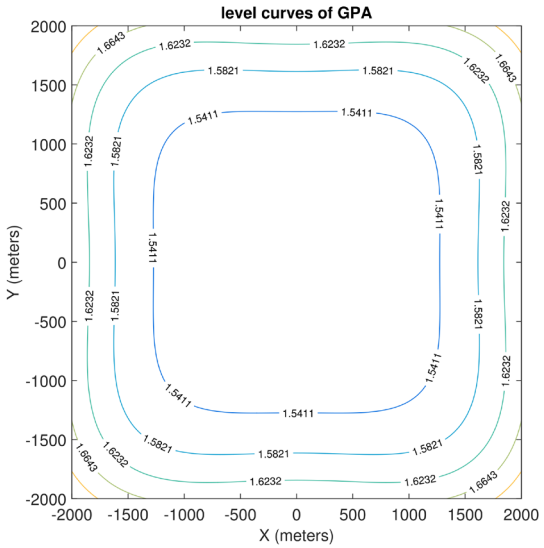

Figure 4: Level curves of HPA in three-dimensional scenarios

From Fig. 3, the best theoretical accuracy can be obtained at the center of beacons. This implies the target around the center of the beacons can achieve more accurate positioning than targets nearby the beacons. As can be seen from Fig. 4, in the three-dimensional scenario, the area with better positioning is also like a square, similar to the beacon formation. Therefore, the beacons for acoustic positioning should be located outside the region of interest. Moreover, the better performance will be achieved when the distances between beacons are larger, only if the target could receive the signals from all beacons. In the interesting region, GPA shows ideal accuracies in some parts of the interesting region. This fact is of great importance to determine the number of beacons needed or

whether the positioning accuracy over a given area meets user needs.

For each case in the three-dimensional scenario, the minimum and maximum GPA, HPA as well as VPA are computed with the optimal beacon placement. The results are shown in Tab. 1.

Table 1: Results for three different heights of the sampling points

	GPAmin	GPAmax	HPAmin	HPAmax	VPAmin	VPAmax
-1000 m	1.5651	1.9538	1.0607	1.2862	0.9682	1.5811
-2000 m	1.5000	1.7464	1.2247	1.4491	0.8602	1.0000
-3000 m	1.6116	1.9274	1.4577	1.6748	0.6872	0.9539

Obviously, it can be shown that the minimum of GPA(GDOP) is obtained when the height of the sampling point is -2000 *m*, and this value satisfied the formula $3/\sqrt{n} = 3/\sqrt{4} = 1.5$. Furthermore, the data in Tab. 1 imply that HPA(HDOP) grows proportional to the height of sampling points. However, VPA(VDOP) increases inversely proportional to the height of sampling points. This conclusion is consistent with the theory in Section 3.2.

5 Conclusions

This paper offers a new characterization of the solutions to assess and optimize the acoustic positioning system. By assuming that the range measurements between the sampling points and the acoustic beacons are corrupted by white Gaussian noise, the assessment parameter DOP related to the positioning accuracy can be derived. Then, the best positioning accuracy to be obtained is converted into that of minimizing the GDOP conveniently. Furthermore, unlike other work only use GDOP to optimize the formation and cannot assess the performance of any specified dimensions whether users satisfy, we apply GPA, HPA and VPA to assess the optimal geometric beacon formation in each dimension for any point in the three-dimensional space. This new assessment model can provide users with guidance advice to optimize performance of each specified dimension. Finally, numerical simulations support the view that the methodology proposed to estimate performance of the acoustic system is feasible. Future work will be aimed at: 1) extending the methodology developed to deal with time bias errors; 2) studying the performance of the acoustic positioning systems in the case of the beacons moving with ocean currents.

Funding Statement: This work was supported by Natural Science Foundation of Hainan Province of China (No. 117212), National Natural Science Foundation of China (Nos. 61633008, 61374007, 61601262 and 61701487), Natural Science Foundation of Heilongjiang Province of China (No. F2017005) and China Scholarship Council.

Conflicts of Interest: The authors declare no conflicts of interest regarding the present study.

References:

Bonin-Font, F.; Ortiz, A.; Oliver, G. (2008): Visual navigation for mobile robots: a survey. *Journal of Intelligent and Robotic Systems*, vol. 53, no. 3, pp. 263-296.

Bayat, M.; Crasta, N.; Aguiar, A. P.; Pascoal, A. M. (2016): Range-based underwater vehicle localization in the presence of unknown ocean currents: theory and experiments. *IEEE Transactions on Control Systems Technology*, vol. 24, no. 1, pp. 122-139.

Chang, L. B.; Li, Y.; Xue, B. Y. (2017): Initial alignment for a doppler velocity log-aided strapdown inertial navigation system with limited information. *IEEE-ASME Transactions on Mechatronics*, vol. 22, no. 1, pp. 329-338.

Cheng, X. Z.; Shu, H. N.; Liang, Q. L. (2008): Silent positioning in underwater acoustic sensor networks. *IEEE Transactions on Vehicular Technology*, vol. 57, no. 3, pp. 1756-1766.

Eustice, R. M.; Pizarro, O.; Singh, H. (2008): Visually augmented navigation for autonomous underwater vehicles. *IEEE Journal of Oceanic Engineering*, vol. 33, no. 2, pp. 103-122.

Levanon, N. (2000): Lowest gdop in 2-D scenarios. *IET Radar, Sonar & Navigation*, vol. 147, no. 2, pp. 149-155.

Moreno-Salinas, D.; Pascoal, A. M.; Aranda, J. (2013): Optimal sensor placement for multiple target positioning with range-only measurements in two-dimensional scenarios. *Sensors*, vol. 13, no. 8, pp. 10674-10710.

Martínez, S.; Bullo, F. (2006): Optimal sensor placement and motion coordination for target tracking. *Automatica*, vol. 42, no. 4, pp. 661-668.

Moreno-Salinas, D.; Pascoal, A. M.; Alcocer, A.; Aranda, J. (2010): Optimal sensor placement for underwater target positioning with noisy range measurements. *IFAC Proceedings Volumes*, vol. 43, no. 20, pp. 85-90.

Moreno-Salinas, D.; Pascoal, A. M.; Aranda, J. (2011): Optimal sensor placement for underwater positioning with uncertainty in the target location. *IEEE International Conference on Robotics and Automation*, pp. 2308-2314.

Moreno-Salinas, D.; Pascoal, A. M.; Aranda, J. (2013): Sensor networks for optimal target localization with earings-only measurements in constrained three-dimensional scenarios. *Sensors*, vol. 13, no. 8, pp. 10386-10417.

Moreno-Salinas, D.; Pascoal, A. M.; Aranda, J. (2014): Optimal sensor trajectories for mobile underwater target positioning with noisy range measurements. *19th IFAC World Congress*, vol. 47, pp. 5139-5144.

Moreno-Salinas, D.; Pascoal, A. M.; Aranda, J. (2016): Optimal sensor placement for acoustic underwater target positioning with range-only measurements. *IEEE Journal of Oceanic Engineering*, vol. 41, no. 3, pp. 620-643.

Rice, H.; Kelmenson, S.; Mendelsohn, L. (2004): Geophysical navigation technologies and applications. *PLANS. Position Location and Navigation Symposium*, pp. 618-624.

Rajasekhar, C.; Dutt, V.; Rao, G. (2015): Investigation of best satellite-receiver geometry to improve positioning accuracy using GPS and IRNSS combined constellation over Hyderabad region. *Wireless Personal Communications*, vol. 88, no. 2, pp. 1-9.

Su, J.; Sheng, Z. G.; Xie, L. B.; Li, G.; Liu, A. X. (2019): Fast splitting-based tag identification algorithm for anti-collision in uhf RFID system. *IEEE Transactions on Communications*, vol. 67, no. 3, pp. 2527-2538.

Su, J.; Sheng, Z. G.; Liu, A. X.; Han, Y.; Chen, Y. (2019): A group-based binary splitting algorithm for UHF RFID anti-collision systems. *IEEE Transactions on Communications*, pp. 1-14 (in press).

Su, J.; Sheng, Z. G.; Leung, V. C. M.; Chen, Y. (2019): Energy efficient tag identification algorithms for RFID: survey, motivation and new design. *IEEE Wireless Communications*, vol. 26, no. 3, pp. 118-124.

Su, J.; Sheng, Z. G.; Liu, A. X.; Fu, Z. J.; Chen, Y. (2020): A time and energy saving based frame adjustment strategy (TES-FAS) tag identification algorithm for UHF RFID systems. *IEEE Transactions on Wireless Communications*, pp. 1-13.

Shabani, M.; Gholami, A.; Davari, N. (2014): Asynchronous direct kalman filtering approach for underwater integrated navigation system. *Nonlinear Dynamics*, vol. 80, no. 1-2, pp. 71-85.

Swaszek, P. F.; Hartnett, R. J.; Seals, K. C. (2017): Lower bounds ondop. *Journal of Navigation*, vol. 70, pp. 1-21.

Teixeira, F. C. (2013): Novel approaches to geophysical navigation of autonomous underwater vehicles. *Fourteenth International Conference on Computer Aided Systems Theory*, pp. 349-356.

Wang, W.; Lv, C. C.; Li, X. (2013): Assessment models and rules of GNSS interoperability. *Advanced Materials Research*, vol. 846, pp. 808-811.

Xu, J. N.; He, H. Y.; Qin, F. J.; Chang, L. B. (2017): A novel autonomous initial alignment method for strapdown 302 inertial navigation system. *IEEE Transactions on Instrumentation and Measurement*, vol. 66, no. 9, pp. 2274-2282.

Xue, Y.; Xu, L. Y.; Yu, J.; Zhang, G. W. (2018): A hot event influence scope assessment method in cyber-physical space for big data application. *Intelligent Automation and Soft Computing*, vol. 24, no. 1, pp. 97-105.

Zhang, T.; Chen, L. P.; Li, Y. (2016): A underwater positioning algorithm based on interactive assistance of SINS and LBL. *Sensors*, vol. 16, no. 42, pp. 1-22.

Zhang, H. (1995): Two-dimensional optimal sensor placement. *IEEE Transactions on Systems, Man, and Cybernetics*, vol. 25, no. 5, pp. 781-792.

Zhang, H. Y.; Chen, G. L.; Li, X. W. (2019): Resource management in cloud computing with optimal pricing policies. *Computer Systems Science and Engineering*, vol. 34, no. 4, pp. 249-254.

Zou, Y. J.; Wang, C.; Zhu, J. S.; Li, Q. Q. (2017): Optimal sensor configuration for positioning seafloor geodetic node. *Ocean Engineering*, vol. 142, pp. 1-9.